12th ICAS Congress
October 12-17,1980
München

Preprint of paper 13.1:

DELTA CANARD CONFIGURATION AT HIGH ANGLE OF ATTACK

by

W. KRAUS

MESSERSCHMITT-BÖLKOW-BLOHM GmbH
Unternehmensbereich Flugzeuge
Postfach 80 11 60
8000 München-Ottobrunn, West-Germany

CONTENTS

Notation

C_h	hingemoment coefficient
C_l	rolling moment coefficient
C_{l_β}	lateral stability
C_m	pitching moment coefficient
C_n	yawing moment coefficient
C_{n_β}	directional stability
$C_{n_{\beta dyn}}$	directional departure parameter
C_N	normal force coefficient
LCDP	lateral control departure parameter
n_z	load factor
M	Mach number
H	altitude
X_{cg}	center of gravity
α	angle of attack
β	side slip angle
δ_a	aileron deflection angle
δ_C	canard deflection angle
δ_{flap}	flap deflection angle l.e.: leading edge t.e.: trailing edge
δ_r	rudder deflection angle
φ	leading edge sweep

References

[1] JOHN H., KRAUS W.
High Angle of Attack Characteristics of Different Fighter Configurations
Symposium on High A.O.A. Aerodynamics, AGARD
4-6 Oct 1978, Sandefjord, Norway

[2] WEISSMAN R.
Preliminary Criteria for Predicting Departure Characteristics / Spin Susceptibility of Fighter-Typ Aircraft
J.Aircraft, Vol. 10, No. 4

1. INTRODUCTION

In the last years it was repeatedly shown by air to air dogfight simulation, how useful the high angle of attack regime is. In figure 1 this area of poststall utilisation is indicated. Sustained maneuvers in poststall regime ($\alpha > \alpha_{max}$) only can be flown at Machnumbers lower than 0.3, because of lack of engine power. Instantaneous maneuvers however, which can give an improvement of shooting position, only have a limitation by the maximum structural limit ($n_z \leqq 9g$). Therefore useful angles of attack are between 25° and 90° for Machnumbers between 0.3 and 1.0, dependent of altitude. As indicated in fig. 1, the area of poststall utilisation is tremendous.

Figure 2 shows a delta canard configuration, which was chosen to get maximum conventional performance in the transonic and supersonic regime. The configuration has the following control devices:

- all movable canard
- leading edge flaps; 4 flaps on each side
- trailing edge flaps; 2 flaps on each side
- poststall flaps
- rudder; one on each side

For this configuration we now pose the requirement for save and coordinated flight in the whole poststall regime.

2. LONGITUDINAL CHARACTERISTICS

It is well known, that induced trim drag is reduced by increasing instability. The margin of instability is limited by the possibilities of trimming and controlling the aircraft. Trimming gives no problems in a wide range of interesting instabilities, neither for the pure delta configuration, nor for the delta canard configuration, see figures 3 and 4.

Figures 5 and 6 show the pitch control of trailing edge flaps and canard. Due to the fact, that pitch down power of canard and flap vanishes at high angles of attack, the minimum pitch down power has to be produced by the basic configuration. This means maximum instability of the total configuration is dictated by the instability contribution of the canard.

3. LATERAL AND DIRECTIONAL CHARACTERISTICS

3.1 Stability

As already shown by JOHN and KRAUS [1], wings with high leading edge sweep may experience lateral instability problems at angles of attack of 25° to 45° due to the formation of strong leading

edge vortices. Since vortex bursting depends on leading edge sweep, the windward vortex bursts earlier than the leeward vortex at yaw conditions and this leads to lateral instability. To get better understanding of this problem, some hinge moment tests at leading edge flaps are analysed (figure 7).

At the inner leading edge flaps (flap no. 4), where the leading edge vortex starts, there are some substantial differences due to yaw angle. The discrete angle of attack, where the maximum hingemoment is reached (break point, where flow separation starts) is shifted proportional to the yaw angle, at the leeward side to higher and at the windward side to lower angles of attack. From some other tests [1] it was known that this lateral instability could be improved by a leading edge flap down deflection. Thereby the bursting of the vortex is moved to higher angles of attack. This is especially true for the pure delta wing, for the delta canard configuration this measure is less effective. Tests pointed out, that for the delta canard it is much more efficient to move the inner part of the l.e. flaps (flap no. 4) upward and the rest of the l.e. flaps down. The improvement can be seen directly at the breakpoint, see figure 8.

Figure 9 shows the influence of the leading edge flap position on lateral stability in presence of the canard. The position -40° for all l.e. flaps gives a slight shift of the instability gap to higher angles of attack, but no reduction of the value of instability. A significant improvement is found by moving the inner leading edge flap up. The explanation for this phenomena is a forced early symmetrical vortex bursting on lee- and windward wing side.

The incidence of the canard has a similar great influence on lateral and directional stability like the l.e. flap position. Lateral stability is influenced by vortex bursting of the canard leading edge vortices in the same manner. Therefore also an analogy to the breakpoint of the canard hingemoment exists, see figure 10. The breakpoint is here the point, where the linear characteristic of the hingemoment ends. Again here on the canard we have earlier vortex burst on the windward side as on the leeward side. This canard vortex burst has a driving influence on the behaviour of the wing vortices and therefore strong effects on lateral stability of the total configuration. The influence of the canard deflection on lateral stability confirms this (figure 11). Especially for canard position δ_C = -20° there is a big change to worse, the instability gap reaches from 22° to 43° angle of attack. However for canard angles δ_C = -40° and -60° there is for trim positions ($\alpha \approx 40° \rightarrow 60°$) a small improvement.

For directional stability at canard position δ_C = -20° there is also a slight worsening at trim positions, but at high angle of attack there is a significant improvement for trim cases. Above 40° angle of attack one can reach the "canard off" curve and obtains again directional stability, in spite of the fact, that the vertical tails are in separated flow behind the body. (This is due to the asymmetric vortex shedding at the "shark nose" of the body).

There are also some strong influences by trailing edge flaps, which are however already described in the paper JOHN/KRAUS [1].

Taking into account all these influences of the different control devices and fulfilling the trim conditions it is possible to find an optimum schedule for lateral and directional stability. With this optimum schedule it is possible to obtain the in figure 12 plotted characteristics, which show full lateral stability and good behaviour of directional stability.

For the "canard off" case it is possible even to get better results, see figure 13. Best values are for l.e. flap deflection -40° and t.e. flap deflection +20°. So an additional possibility could be to have the canard in free floating position to simulate the "canard off" configuration and to obtain their advantages.

For longitudinal trimming and control this is no problem, as shown already before. But comparing the lateral and directional stability of "canard off" with "canard on" for canard positions, where the canard is free-floating for $\beta = 0$ (see fig. 4) there are some small differences, see figure 14. The explanation is, that the free floating canard at yaw conditions can have different free floating angles for right and left side, as shown in figure 15 for two angles of attack. Results of a test with free floating canard again show no satisfactory agreement with the canard off plots, figure 16. The reason may be mainly an unfavourable position of canard pivot axis too close to the center of pressure, which ends up in too small reestablishing moments. One can expect better results by a better adjusting of the pivot axis.

Poor lateral/directional stability characteristics at near- and poststall angles of attack can lead to a high degree of spin susceptibility following departure from controlled flight. There are several parameters, developed by WEISSMAN [2], that are useful in predicting aircraft behaviour in stall region, see figure 17.

The most important parameter for predicting directional departure is generally known as $C_{n_{\beta_{dyn}}}$. If $C_{n_{\beta_{dyn}}}$ becomes negative a yaw departure is possible. If it remains negative over a fairly wide range of angle of attack, a yaw departure is highly probable when the aircraft operates in this region.

Figure 18 shows this parameter for the "canard off" and "canard on" case (for several canard settings). The "canard off" case has positive $C_{n_{\beta_{dyn}}}$ in the whole angle of attack regime. For the "canard on" case the canard $\delta_C = -20°$ is again the worst case.

Taking into account the optimum trim schedule, see figure 19, the $C_{n_{\beta_{dyn}}}$-parameter has only in the region of 35° angle of attack a very small excursion to negative values, so that spin suspectibility can not be expected.

Of great importance is also the behaviour of pitch moment over

yaw angle. To minimize spin suspectibility a pitch down characteristic over ß is favourable to get a decrease of angle of attack, if high yaw angles occur in the stall region. Such a behaviour exists for the delta canard configuration, as figure 20 shows.

3.2 Control

Figure 21 shows roll control for different use of the ailerons. For angles of attack greater 30° the mean part (60% to 80%) of roll control comes from using only ailerons up. By these types of aileron deflection (type E + F) over the whole angle of attack regime proverse yaw moment exists, see figure 22.

So these types seem to be the best one which can be used in the poststall area, only the amount of roll control should be improved. This is done by the poststall flaps (figure 23).

Figure 24 shows the rudder effectiveness of the twin fin. Until 40° angle of attack there is sufficient yaw power together with an adverse roll moment. For higher angles of attack additional yaw power is necessary by other devices, for example by a vectored nozzle.

There are some other WEISSMAN parameters to predict, whether control inputs can lead to departure with spin entry: for aileron the aileron alone departure parameter AADP and for aileron plus rudder the lateral control departure parameter LCDP, see fig. 17. This parameter should be positiv in the whole angle of attack regime, to avoid aileron reversal, which can lead to departure. As shown in figure 25 this is not true for all types of aileron deflections for the angle of attack regime α = 28° to 45°.

A plot of AADP or LCDP versus $C_{n_{\beta_{dyn}}}$ was recommended by WEISSMAN. He indicated in these plot boundaries for spin suspectibility, gained from several model and full scale free flight tests with several different fighter aircrafts, see figure 26. This plot also shows moderate spin suspectibility at 35° angle of attack and low spin suspectibility in the angle of attack regime 28° to 45°.

This behaviour can be improved by using the rudder proportional to sideslip angle in order to reduce sideslip, which is described by the parameter $LCDP_{(K1)}$. A second possibility for improvement is a aileron rudder interconnect, to deflect the rudder proportional to the aileron in order to counter aileron yaw, which is described by LCDP(K2), see fig. 17. For a ratio rudder to yaw angle K1 = 3.0 and a ratio rudder to aileron K2 = 2.5 the improvements can be seen in figure 27. The result is no spin suspectibility in the whole angle of attack regime.

It should be pointed out here very clearly, that these WEISSMAN parameters should only be used during aerodynamic development to get a judgement of aircraft behaviour in stall and poststall regime. Therefore the improvements by aileron rudder

interconnect or rudder yaw angle interconnect only can show that poor LCDP-parameters can be corrected, but they give no statement how to manage a control system properly. In practice it could be shown by flight mechanical analysis that best results are obtained, if the poor directional stability (at stall angles) is corrected by yaw control of a vectored nozzle.

4. CONCLUSIONS

It was shown, that there exists no problem for the configuration in the high angle of attack regime regarding longitudinal characteristics, neither for trimming nor for control.

The lateral stability can be sufficiently improved by a special trim schedule, directional stability is somewhat poor for angle of attacks 30° to 45°. Roll control is good in the whole angle of attack regime, yaw control is lost at 45° angle of attack. Spin suspectibility can be avoided at stall conditions by improving yaw control using a vectored nozzle.

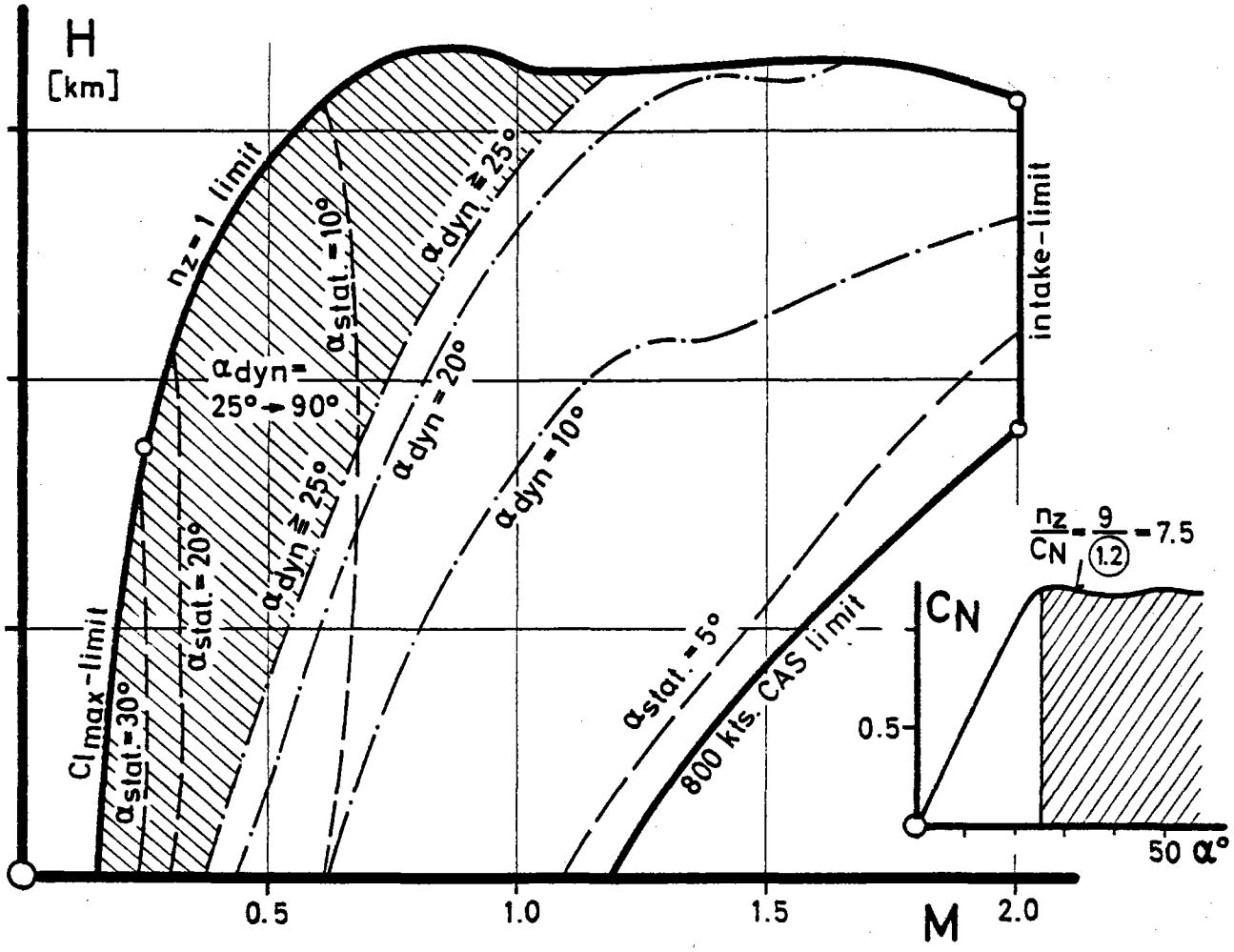

Fig. 1 Flight Envelope

Area of PST-Utilization.
Structural limit $n_z = 9$ for
Instantaneous Maneuvers

FIG. 2 SCHEME OF CONTROL DEVICES ARRANGEMENT ON A DELTA / CANARD CONFIGURATION

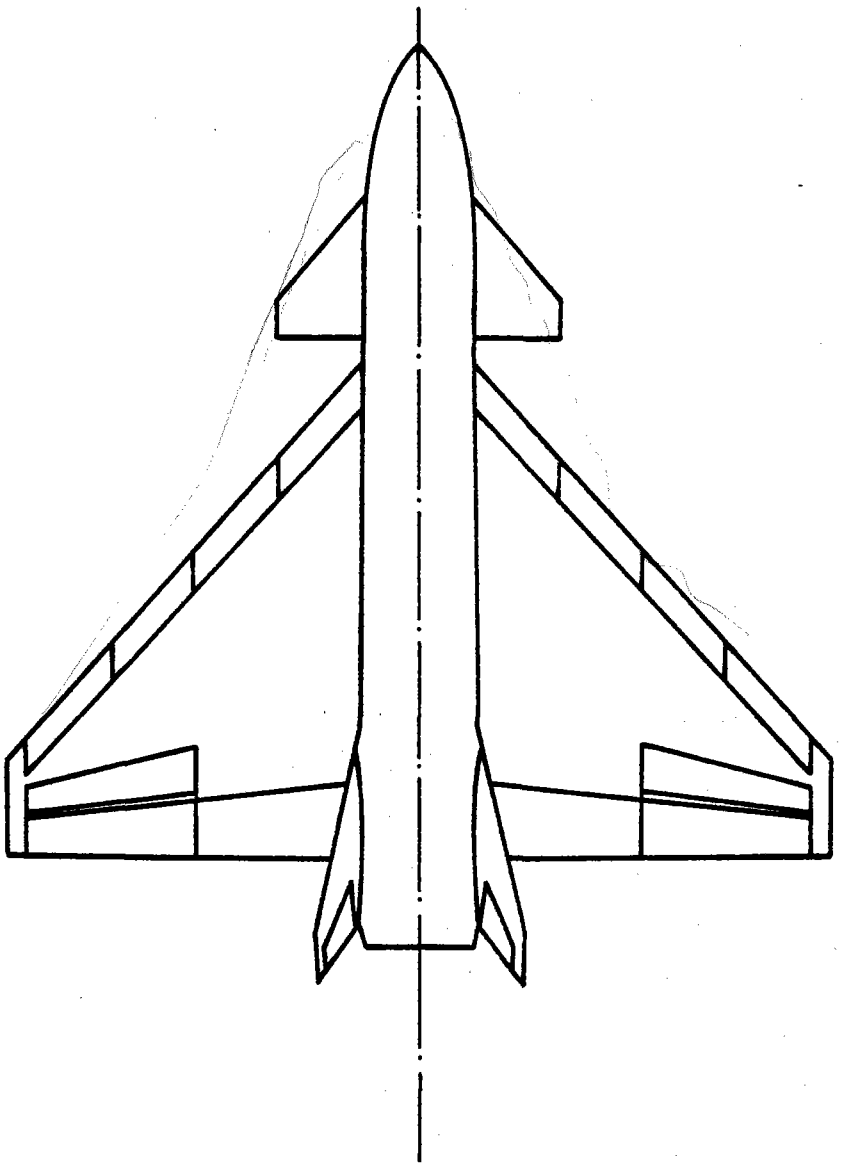

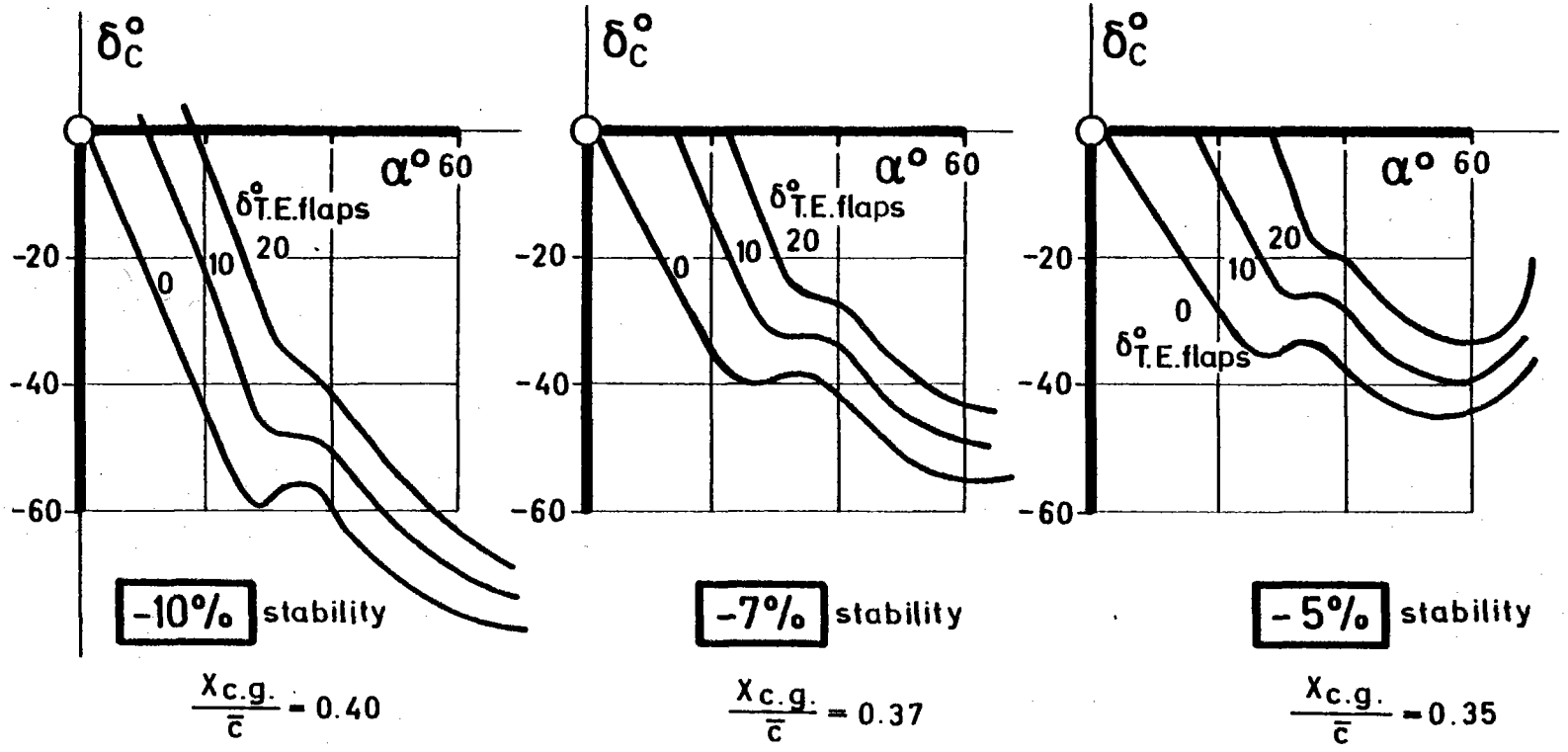

Fig. 3 Trim-Diagram for Delta Canard Configuration

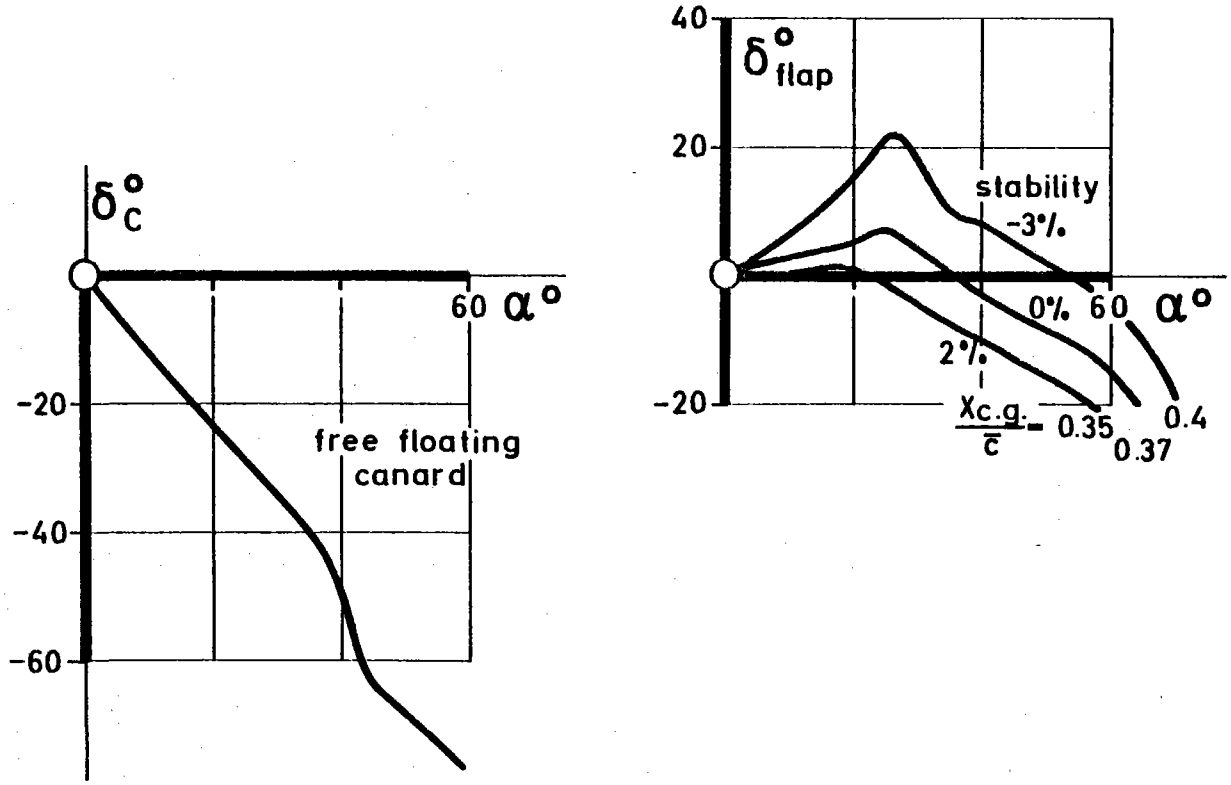

Fig. 4 Trim-Diagram for Delta Alone and for Delta Canard with Free-Floating Canard

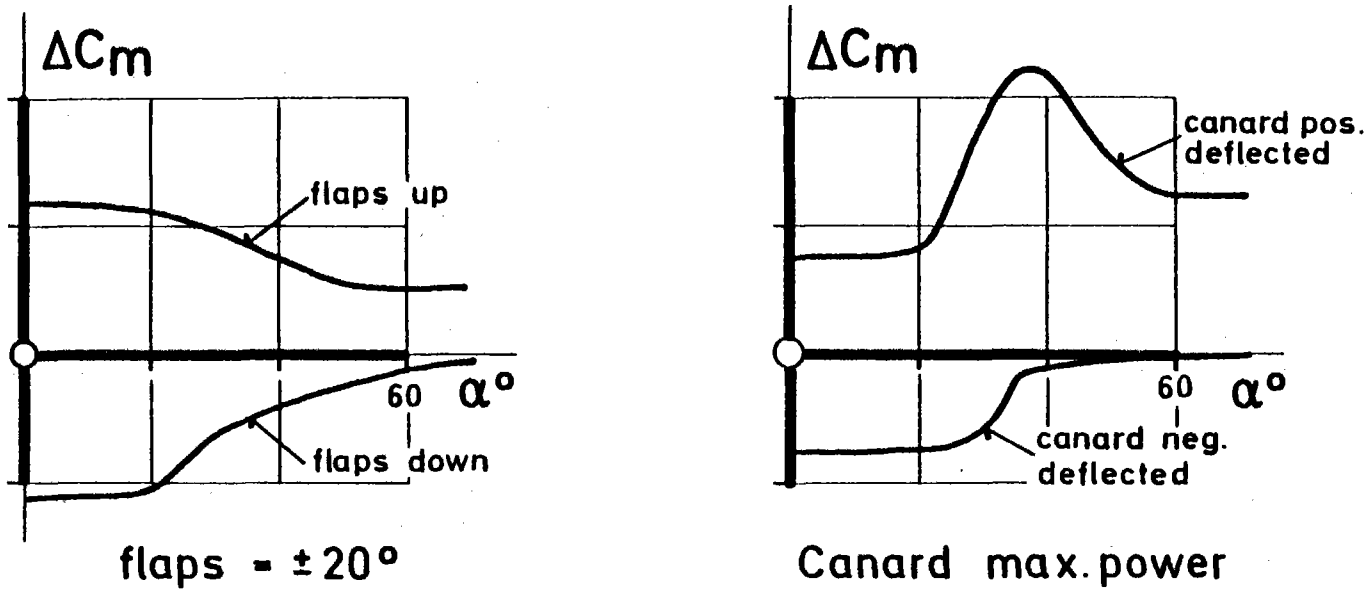

Fig. 5 Pitch Control

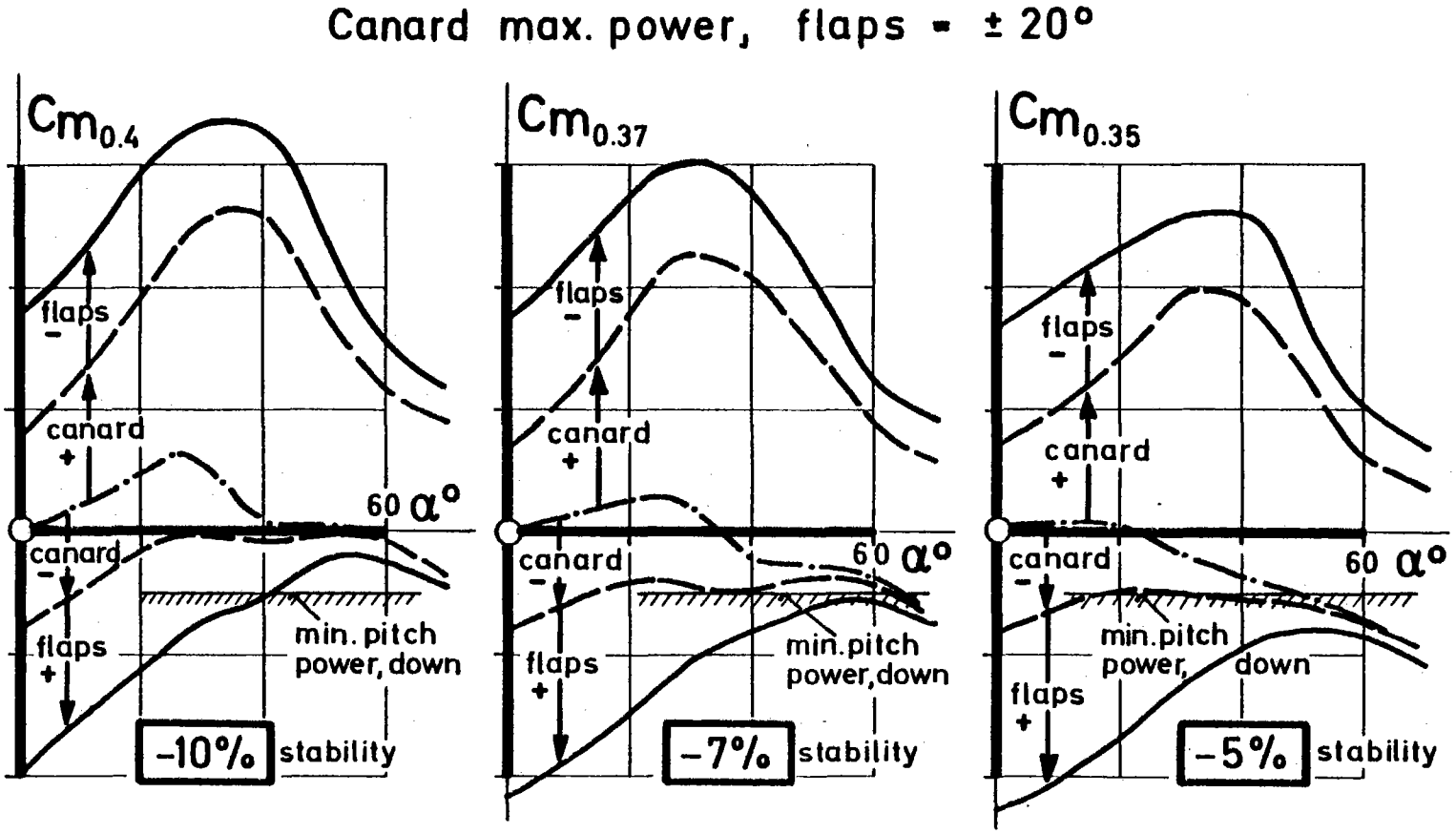

Fig. 6 Max. Pitch Down Control Power, Delta Canard Configuration

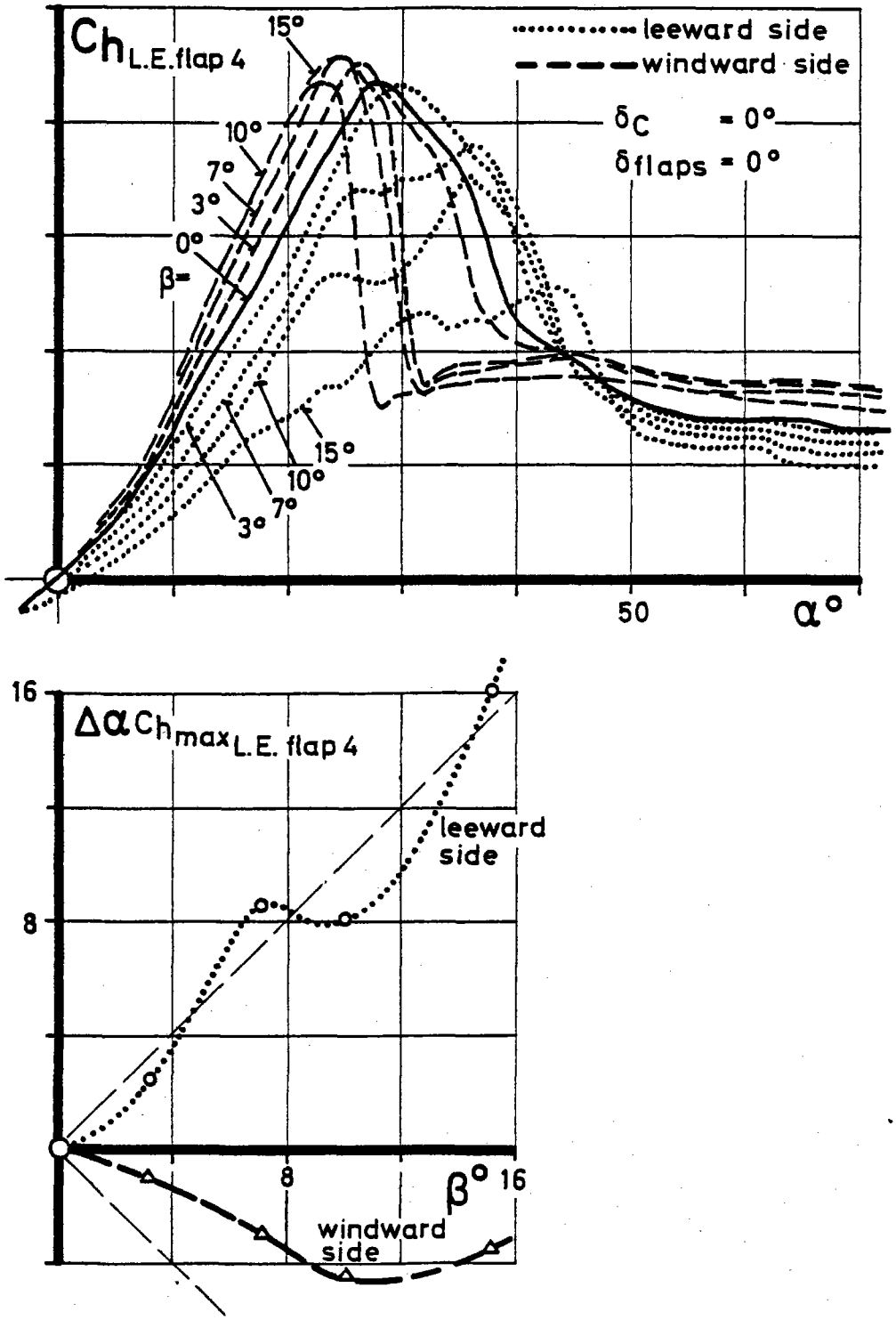

Fig. 7 Hinge Moment at L. E. Flaps

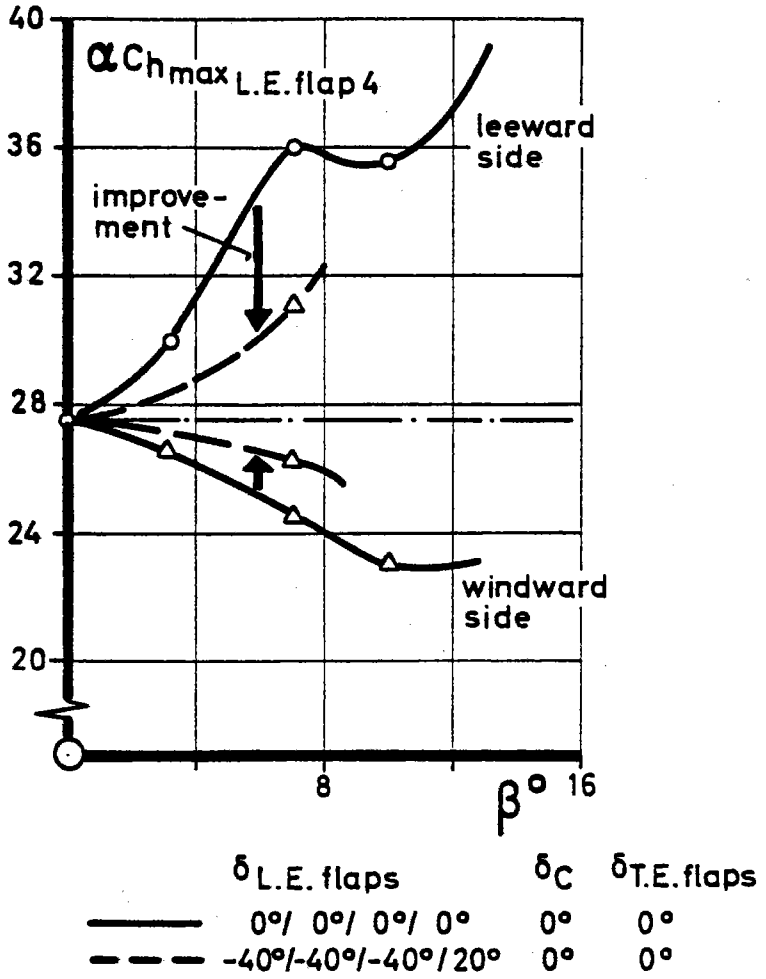

Fig. 8 Angle of Max. Hinge Moment of L.E. Flap No. 4

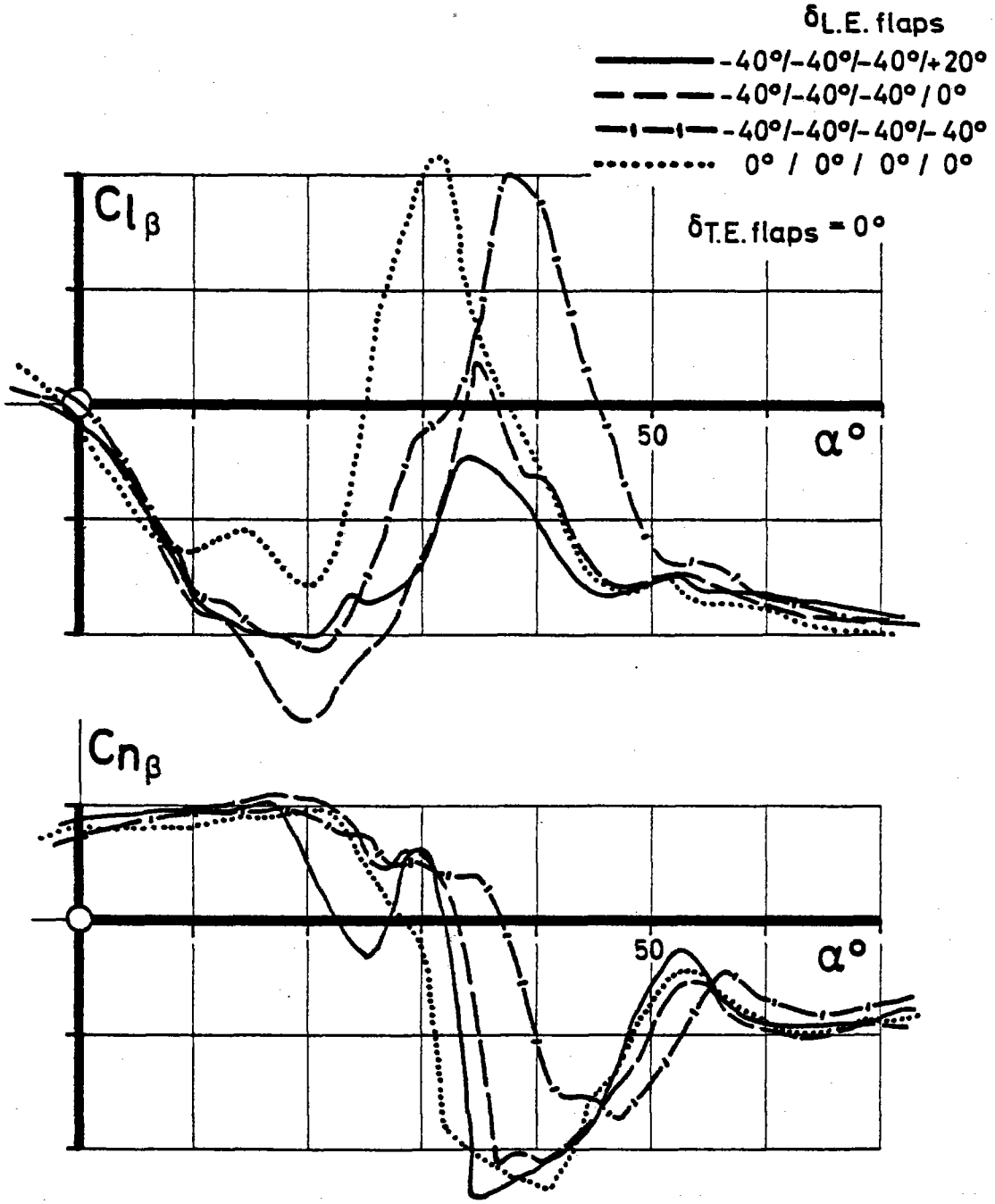

Fig. 9 Influence of L.E. Flaps, Canard on

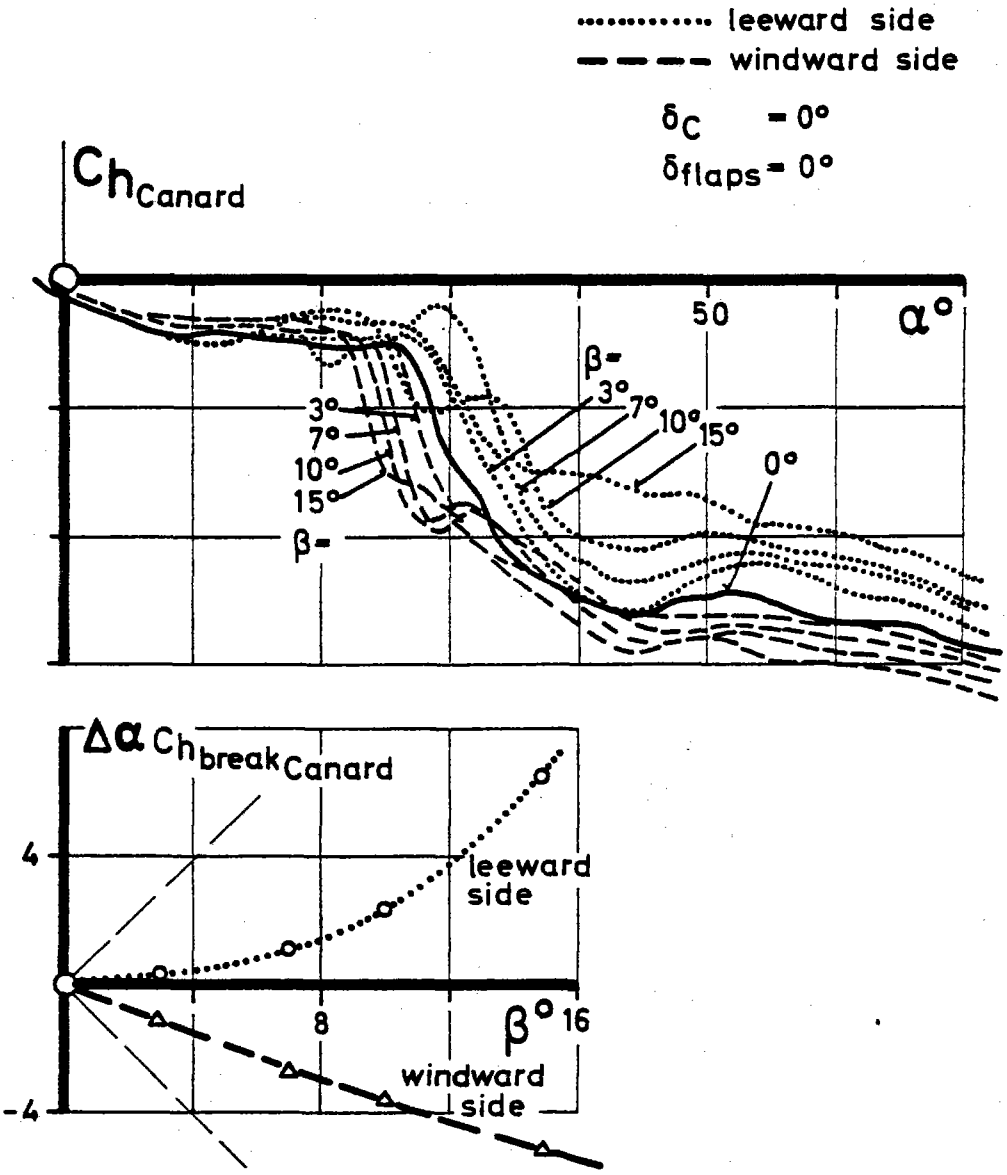

Fig. 10 Hinge Moment at Canard

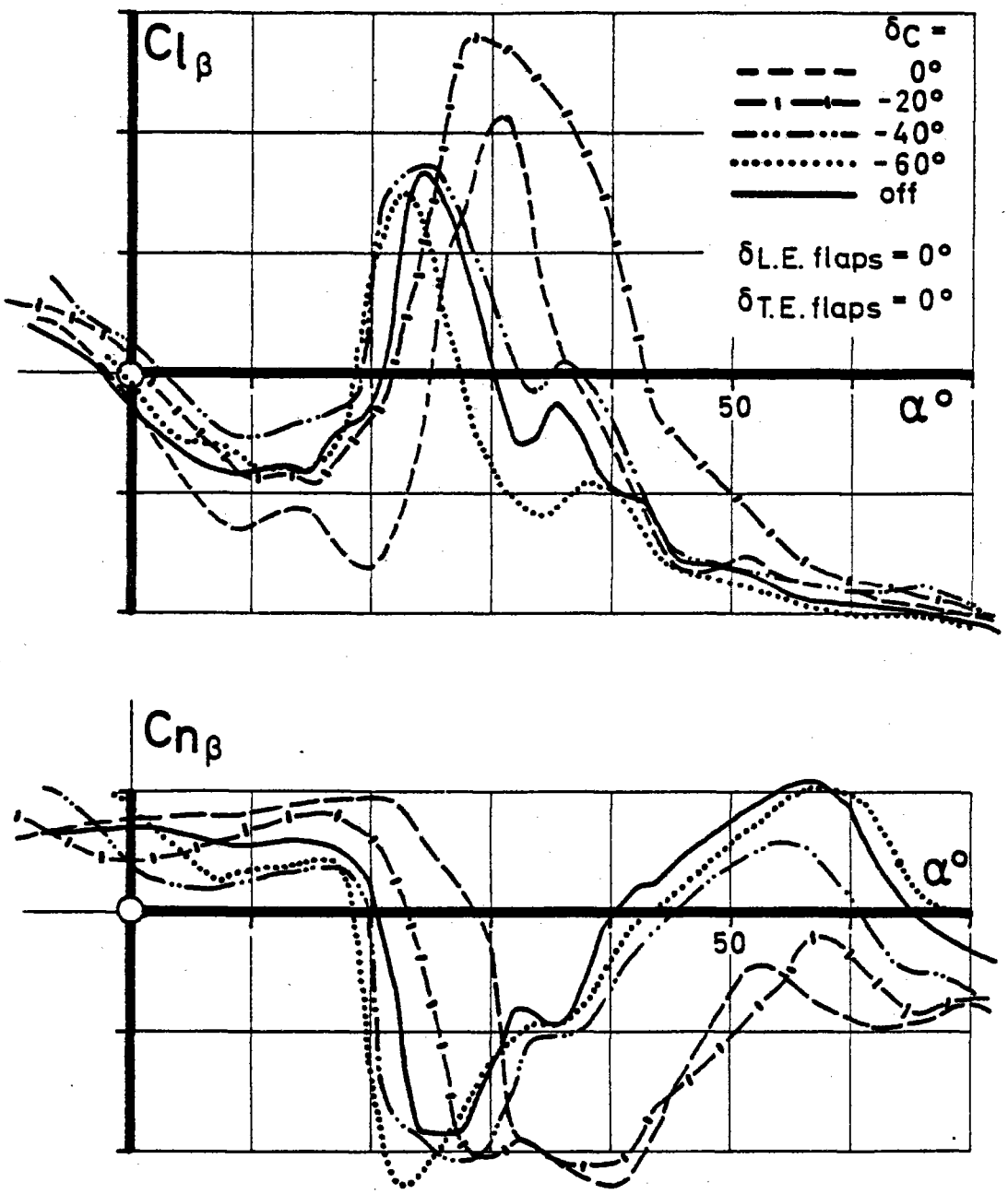

Fig. 11 Influence of Canard Deflection

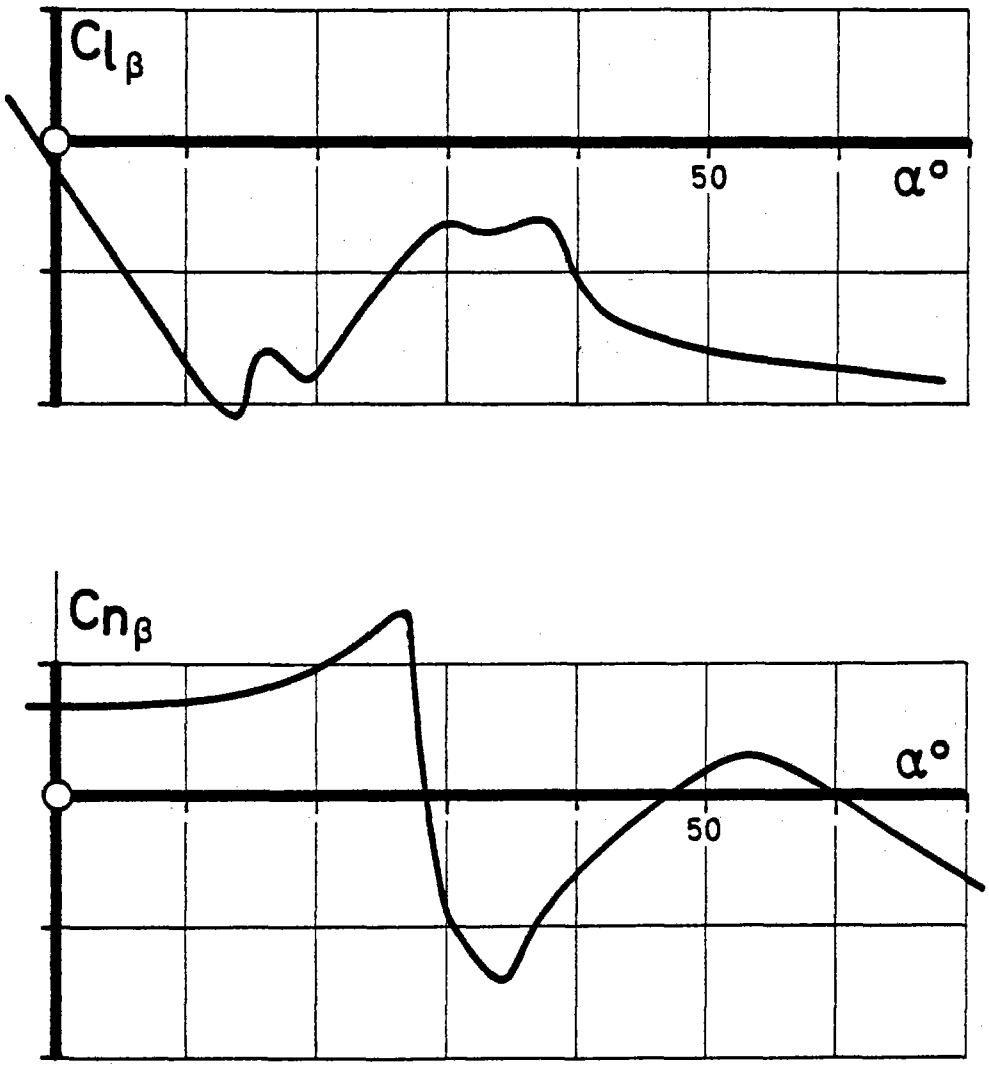

Fig. 12 Optimum Canard, L.E. and T.E. Flap-Deflections for Lateral- and Directional Stability and Trim-Condition

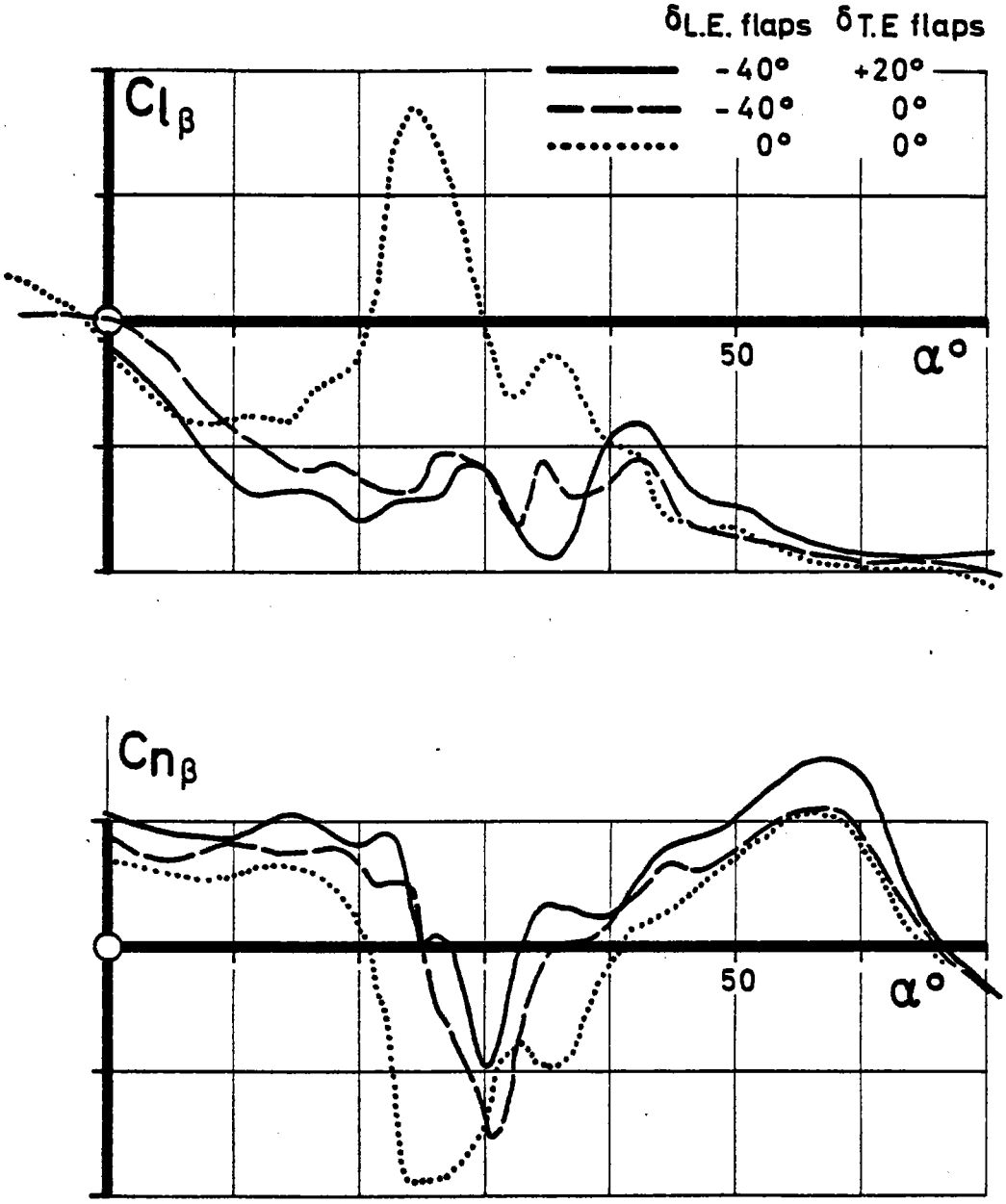

Fig. 13 Influence of Flaps, Canard off

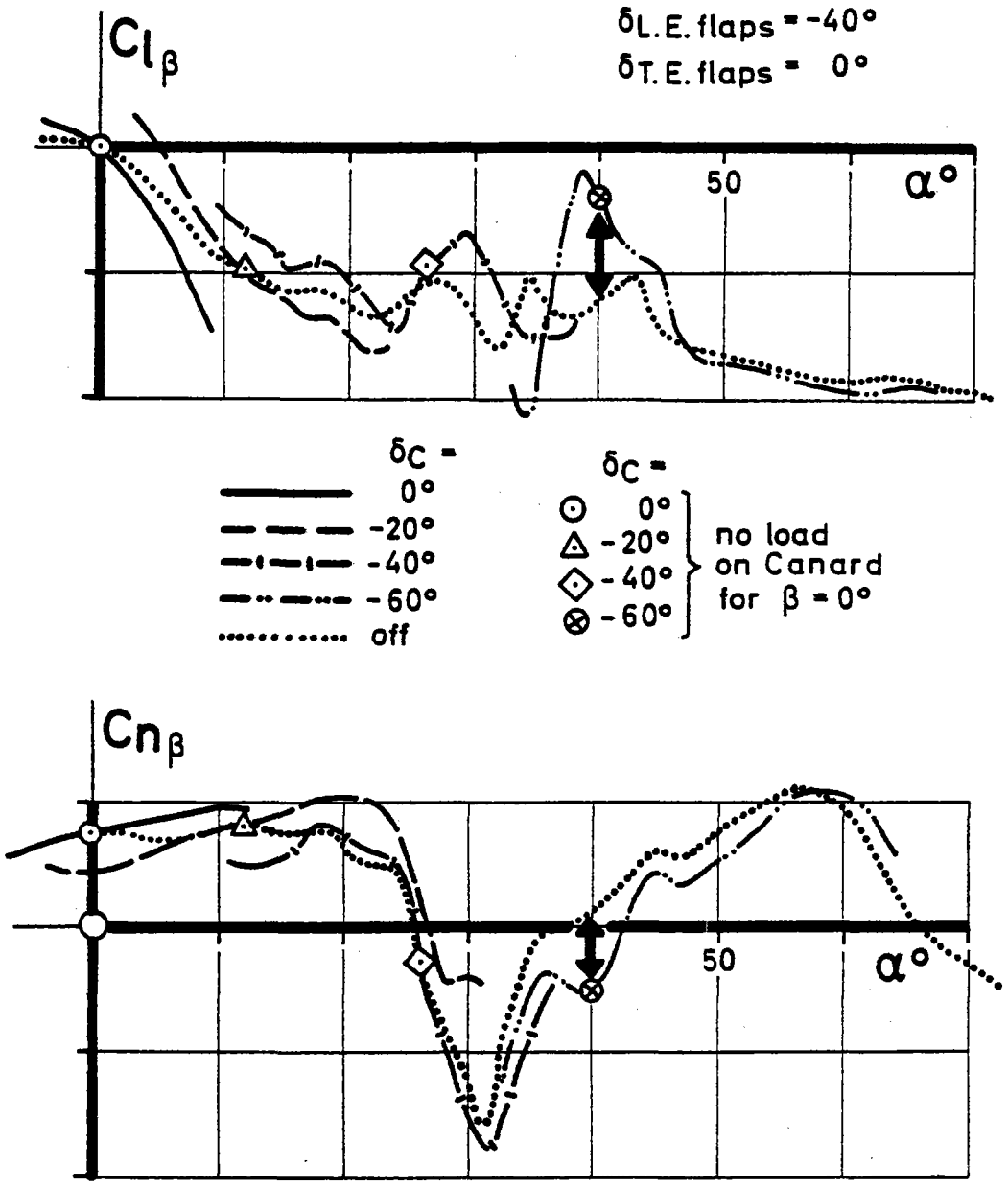

Fig. 14 Floating Canard

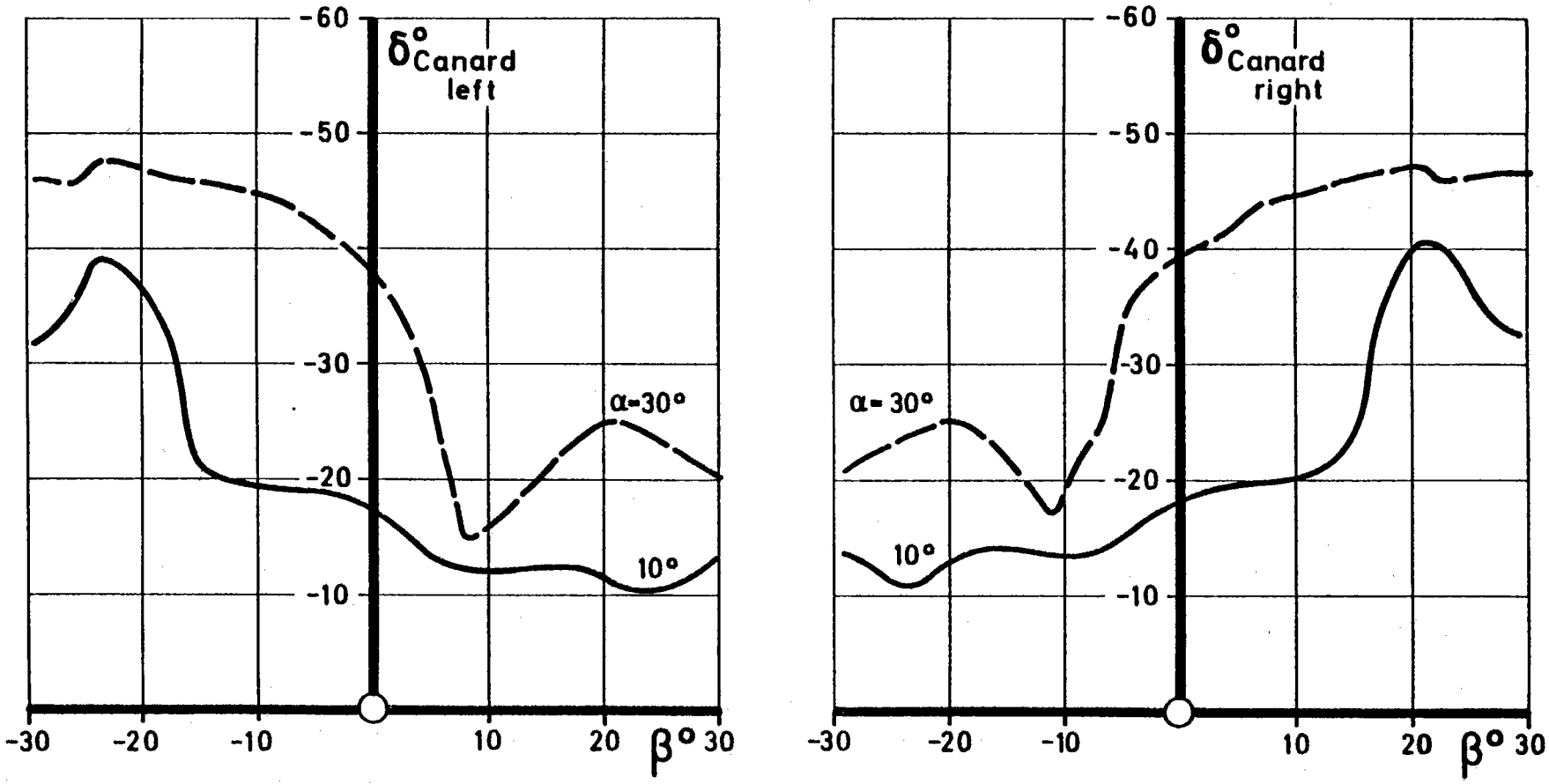

Fig. 15 Free-Floated Canard, Canard Angles

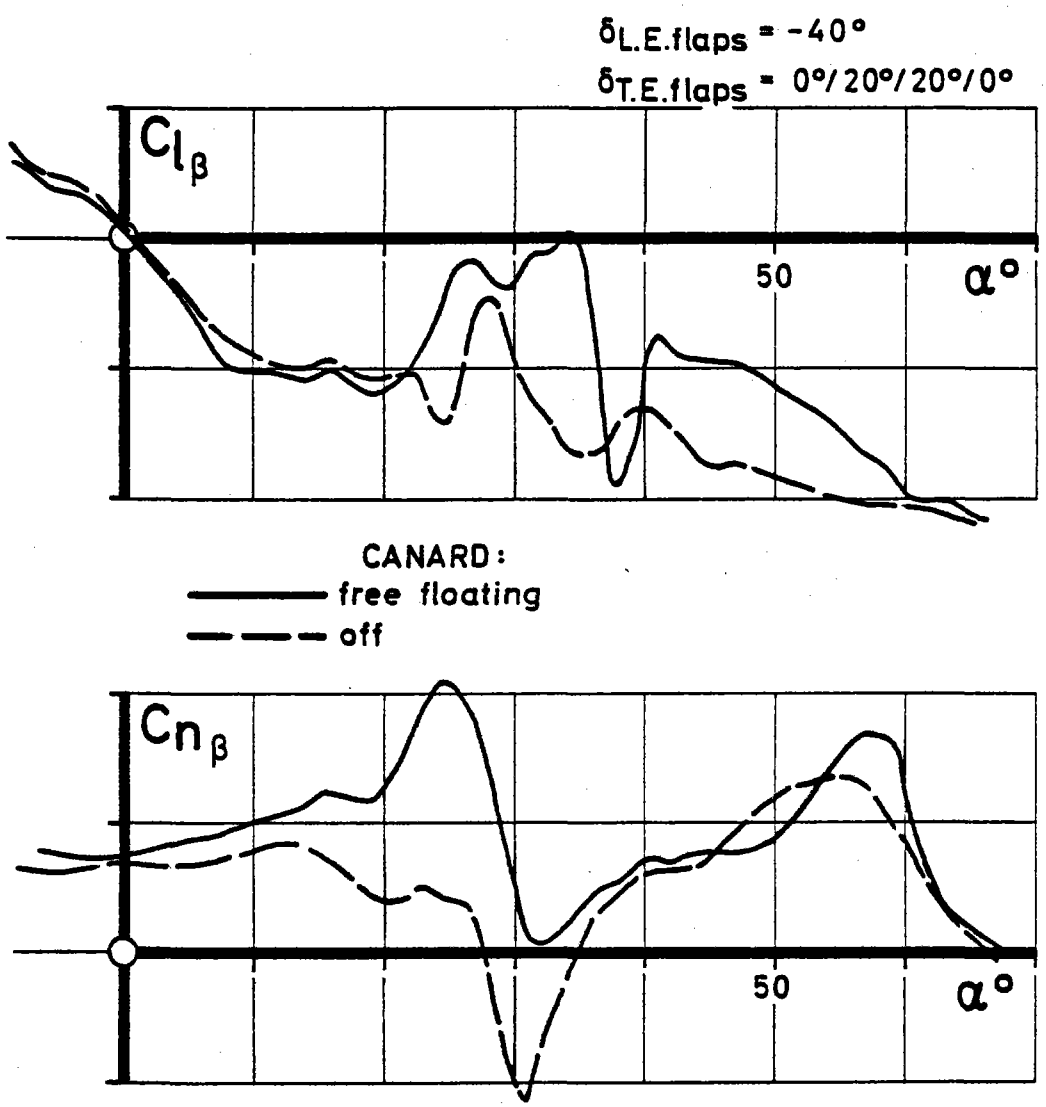

Fig. 16 Free-Floating Canard

DIVERGENCE CRITERIONS

(1) $$C_{n_{\beta dyn}} = C_{n_\beta} \cdot \cos\alpha - \frac{I_z}{I_x} \cdot C_{l_\beta} \sin\alpha$$

(2) Aileron alone departure parameter

$$AADP = C_{n_\beta} - C_{l_\beta} \cdot \frac{C_{n\delta_a}}{C_{l\delta_a}}$$

(3) Lateral control departure parameter for the aileron plus rudder proportional to sideslip

$$\delta_r = - K_1 \cdot \beta$$

$$LCDP_{(K_1)} = C_{n_\beta} - C_{l\beta} \frac{C_{n\delta_a}}{C_{l\delta_a}} + K_1 \cdot \left(\frac{C_{n\delta_a}}{C_{l\delta_a}} C_{l\delta_r} - C_{n\delta_r}\right)$$

(4) Lateral control departure parameter for the aileron plus rudder proportional to aileron

$$\delta_r = K_2 \cdot \delta_a$$

$$LCDP_{(K_2)} = C_{n_\beta} - C_{l_\beta} \cdot \left(\frac{C_{n\delta_a} + K_2 \cdot C_{n\delta_r}}{C_{l\delta_a} + K_2 \cdot C_{l\delta_r}}\right)$$

Fig. 17

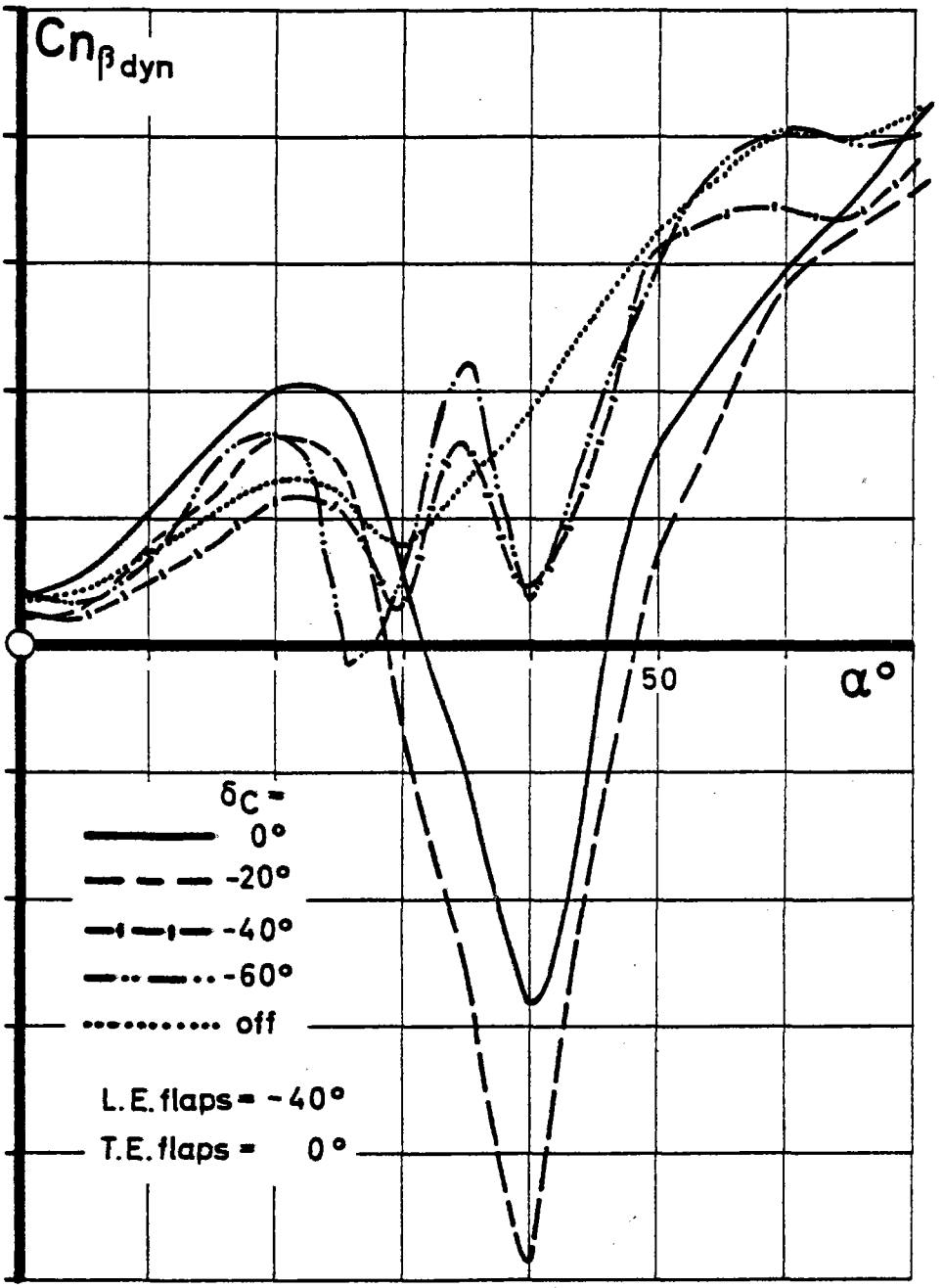

Fig. 18 Cn_β , Dynamic

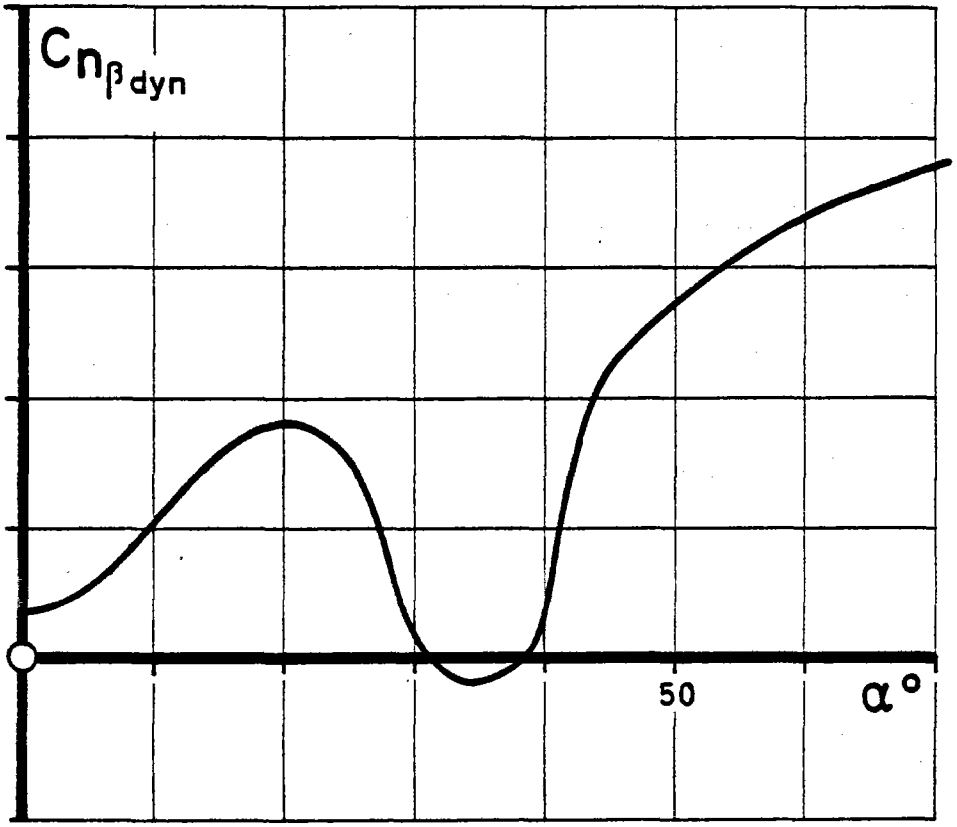

Fig. 19 Optimum Canard, L.E. and T.E. Flap-Deflections for Lateral- and Directional Stability and Trim-Condition

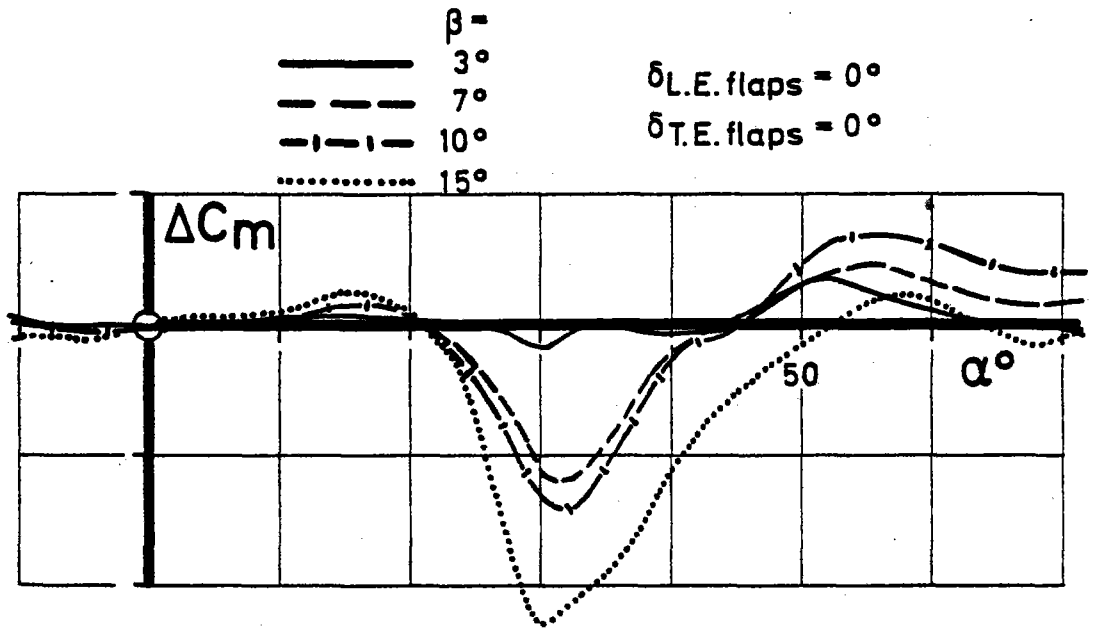

Fig. 20 Influence of Yaw Angles on Pitching Moment

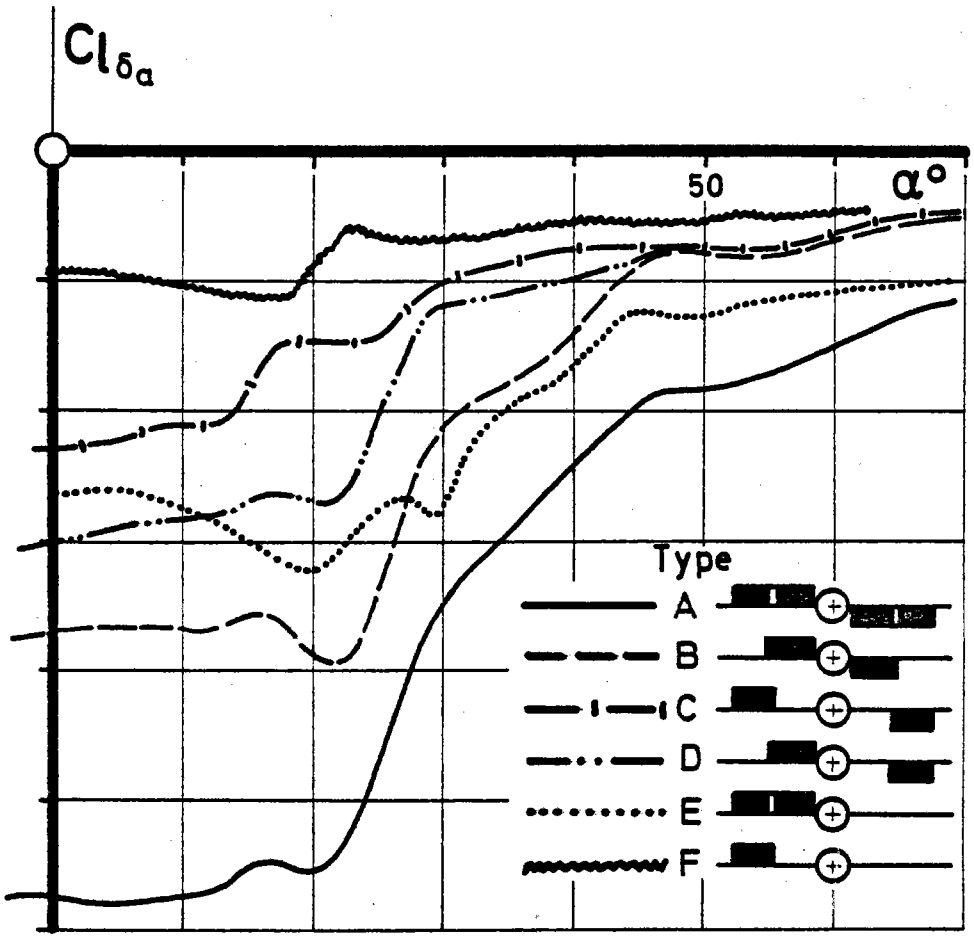

Fig. 21 Roll Control

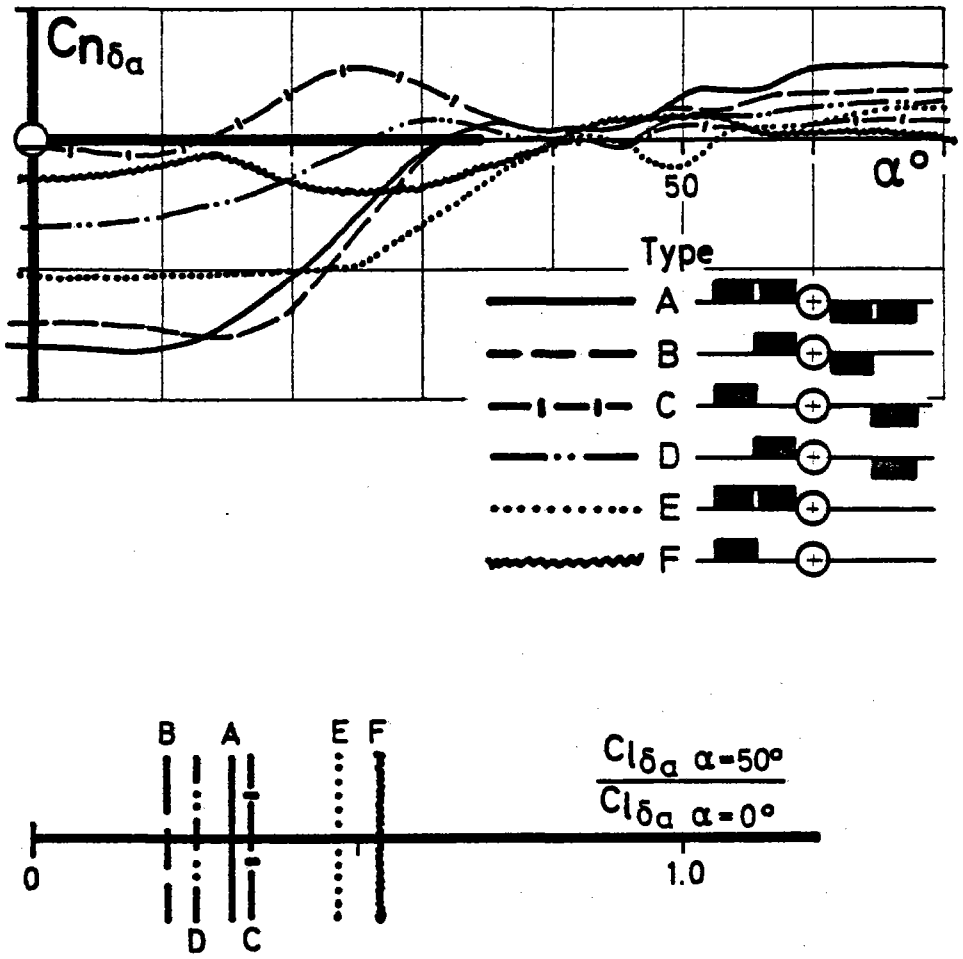

Fig. 22 Roll Control

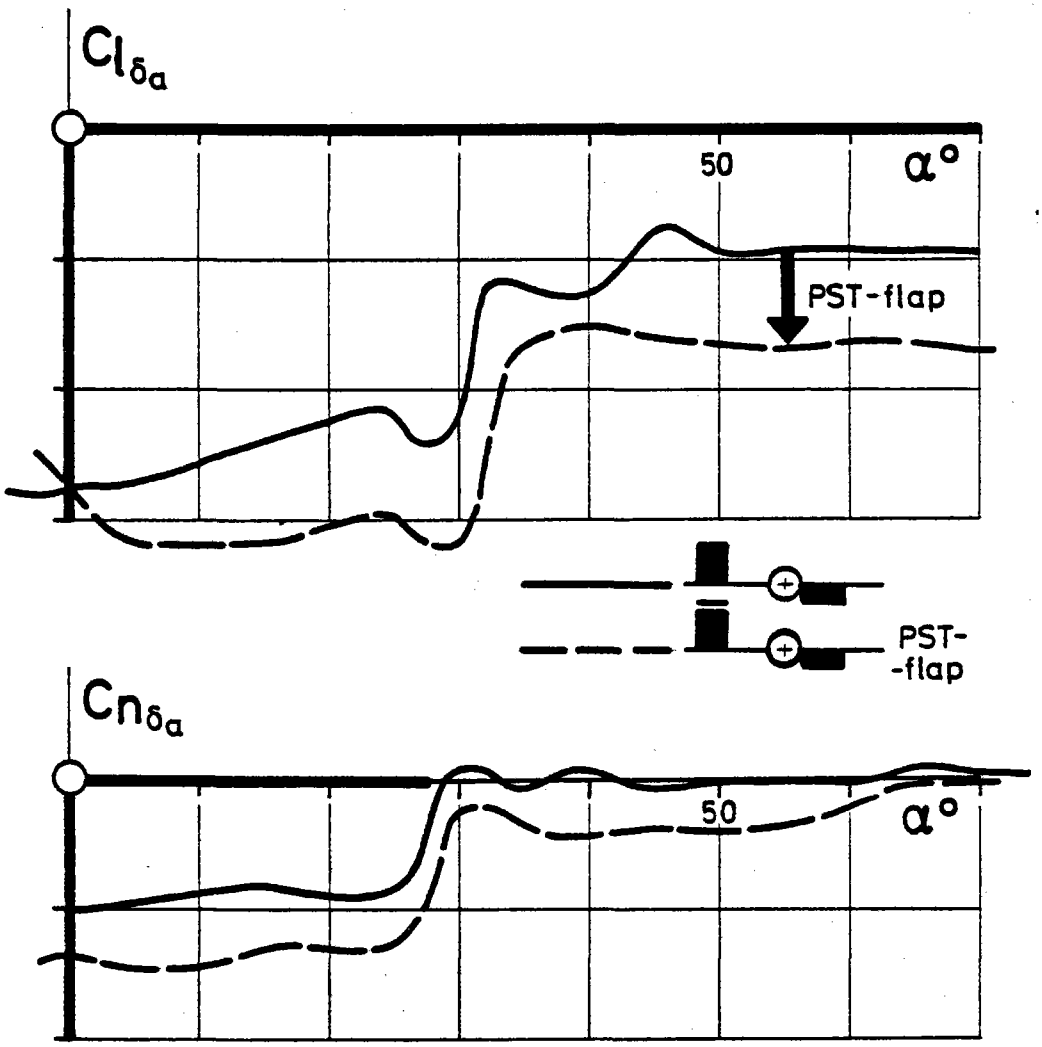

Fig. 23 Roll Control

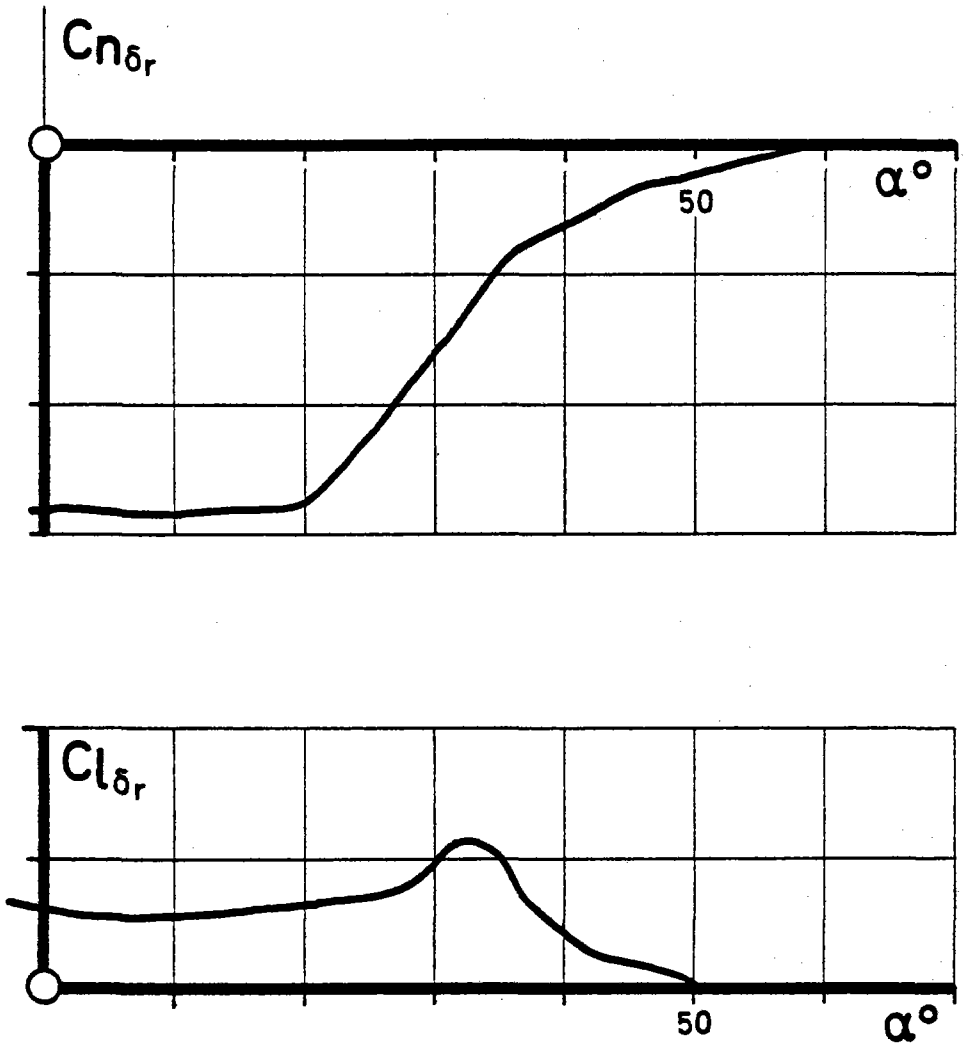

Fig. 24 Yaw Control

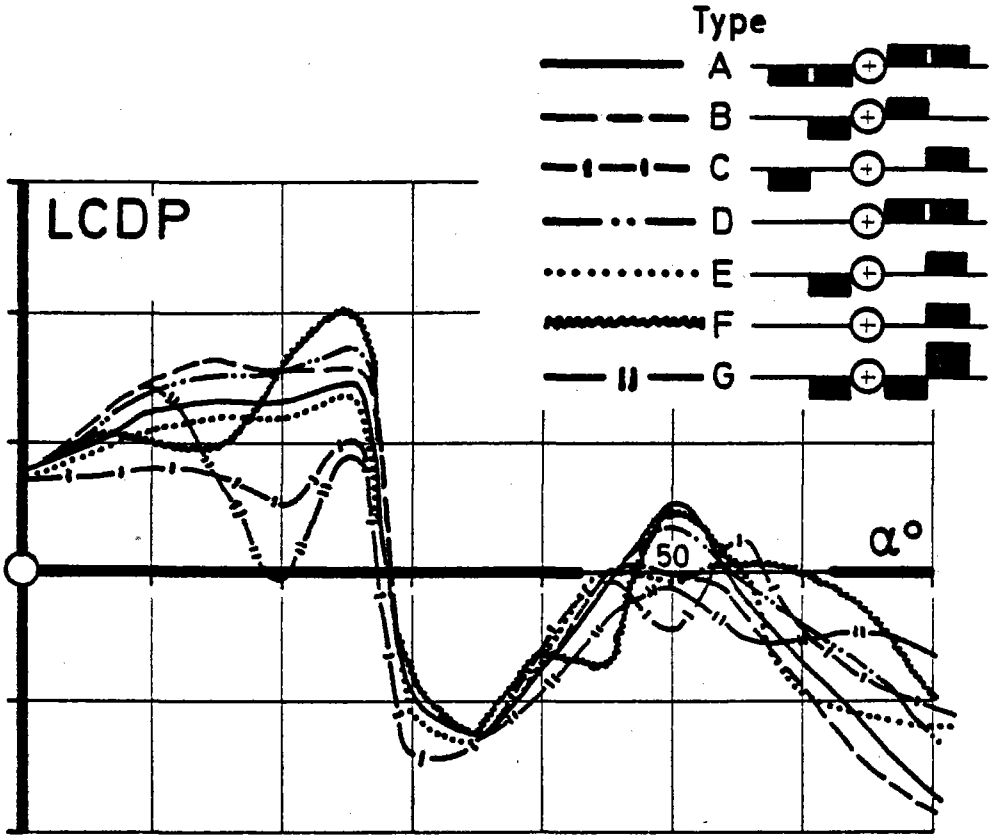

Fig. 25 LCDP

Optimum Canard, L.E. and T.E. Flap - Deflection and Trim - Condition

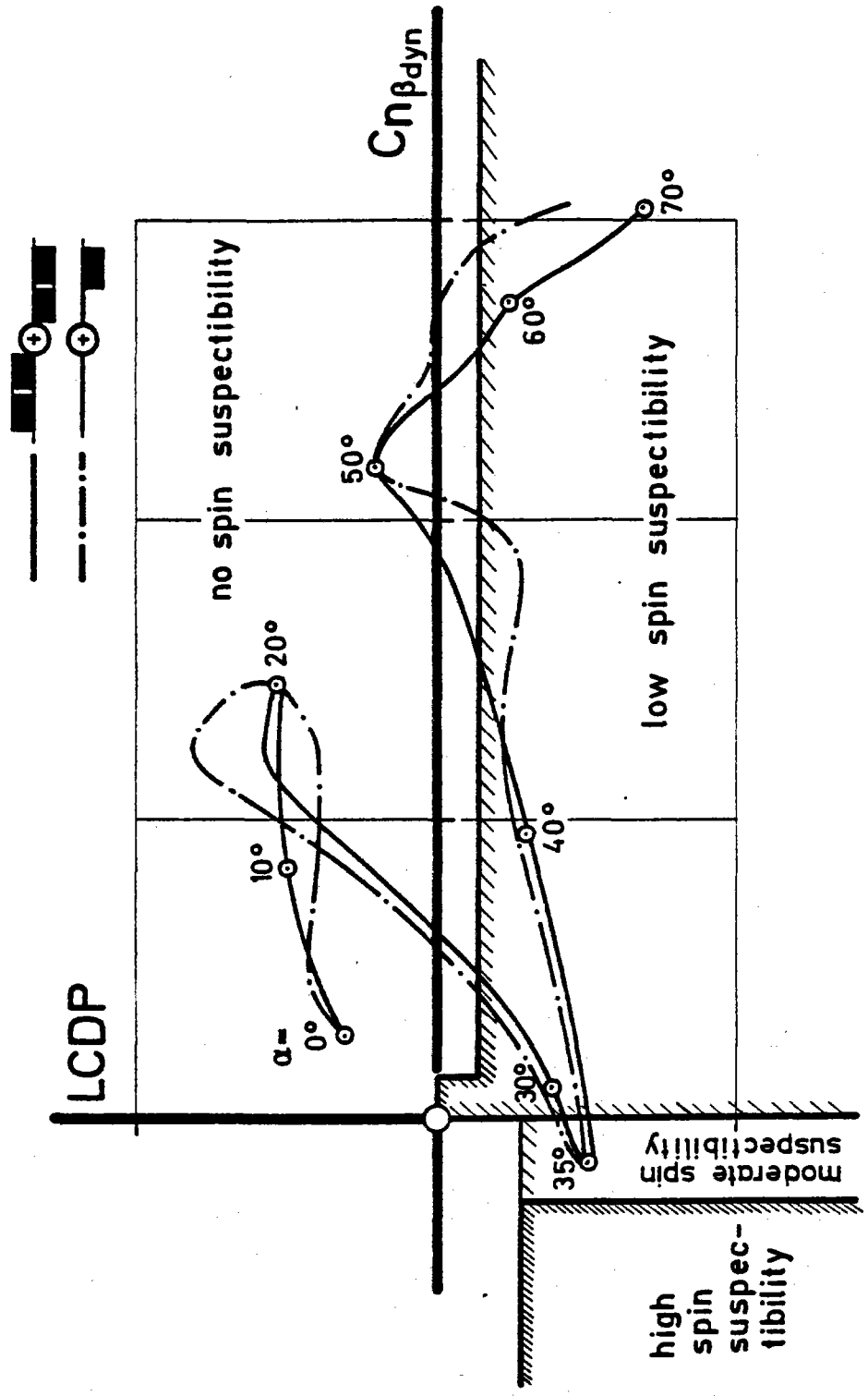

Fig. 26 LCDP

Optimum Canard, L.E. and T.E. Flap-Deflection and Trim-Condition

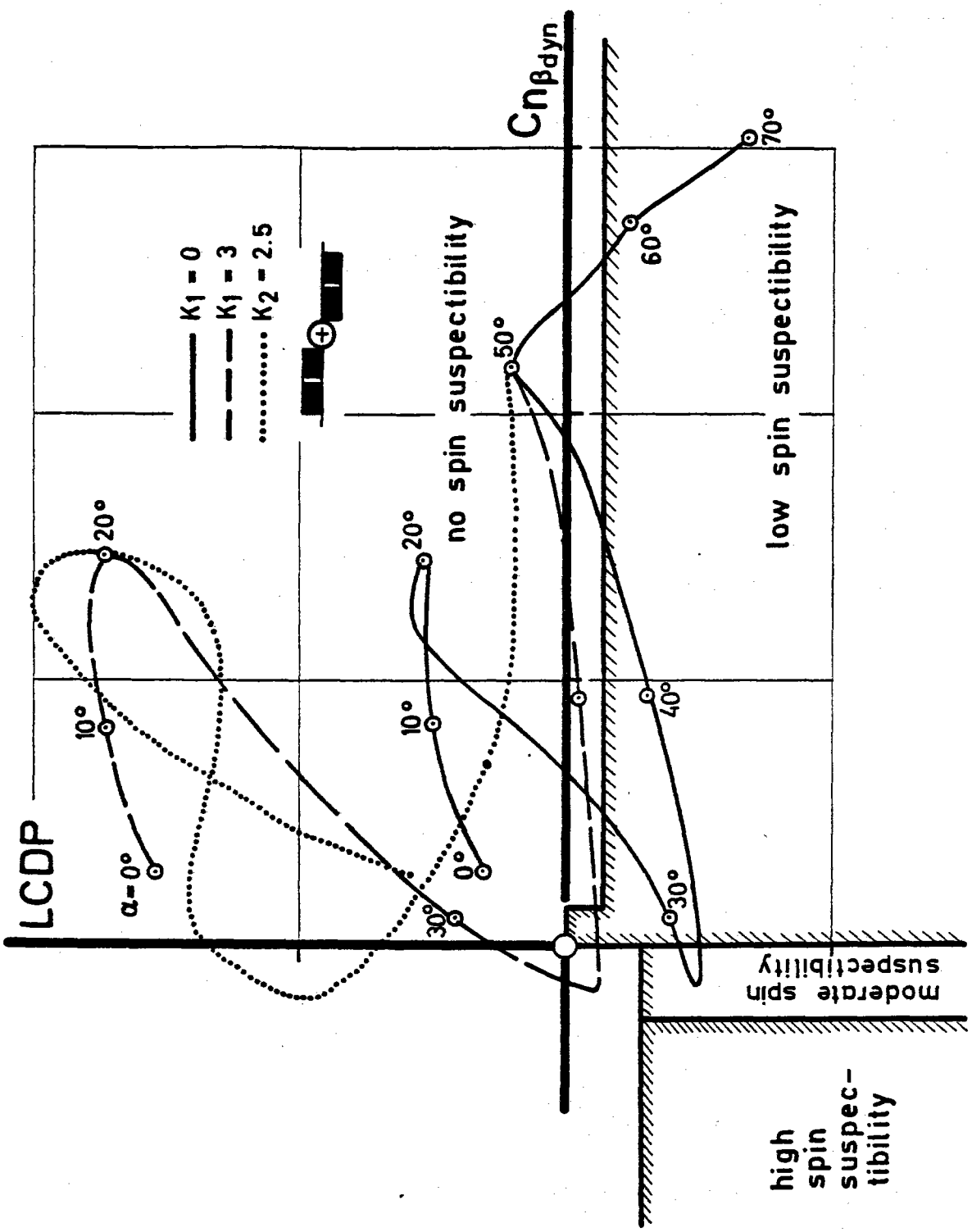

Fig. 27 LCDP

Optimum Canard, L.E. and T.E. Flap-Deflection and Trim-Condition